Electronic supplementary information

Bio-inspired Transparent MXene Electrodes for Flexible UV Photodetector

*Jiaxin Chen, Ziliang Li, Fenglou Ni, Weixin Ouyang, and Xiaosheng Fang**

Department of Materials Science, Fudan University, Shanghai 200438, China

* corresponding authors: xshfang@fudan.edu.cn

S1. Experimental details

Materials

NaOH (96%), HCl (36.0-38.0%), acetate (99.0%), anhydrous ethanol, polydimethylsiloxane (PDMS) are from Sinopharm Chemical Reagent Co., Ltd.. LiF (98.5%, 325 mesh, Alfa Aesar), Ti_3AlC_2 (98%, 400 mesh, 11 Technology Co., Ltd.), HF (49 wt%, Macklin), tetrabutylammonium hydroxide (TBAOH, 54.0-56.0%, Sigma), polyvinylpyrrolidone (PVP, M_{ave}=1300000, Aladdin), titanium (IV) isopropoxide (95%, Aladdin)

Synthesis of leaf vein networks

The leaves were etched in boiling 0.1 g mL^{-1} NaOH solution for several hours, after that the mesophyll was brushed off the vein. Then the leaf vein was dried in a 60℃ oven, pressed with a piece of glass to keep flat.

Synthesis of m-$Ti_3C_2T_x$

The synthesis process was according to the literature.[1] 1g LiF was added to 20 mL 9 M HCl solution and the solution was stirred for 30 min. Then 1 g Ti_3AlC_2 powder was slowly added into the solution in 5 minutes and the solution was stirred at 40℃ for 24 hours. After etching, the resultant solution was washed via centrifugation (10 min at 3500 rpm), then the supernatant was decanted into waste, followed by the addition of DI water and 5 min hand-shaking. The washing process was repeated several times until the supernatant became dark-green and the pH was around 6. After collecting the supernatant, the black slurry of m-$Ti_3C_2T_x$ could be used to coating the leaf. The MXene solutions in Figure S1 were prepared by adding DI of various volumes into acquired m-$Ti_3C_2T_x$ slurry.

Synthesis of h-$Ti_3C_2T_x$

The synthesis process was according to the literature.[1] 1 g Ti_3AlC_2 powder was slowly added into HF and stirred for 3 hours at room temperature. The solution was washed several times via centrifugation until the pH was about 6. Then the precipitate was dried in vacuum at 80℃ for 12 hours. TBAOH was added to the obtained powder in the proportion of 10 mL per gram. The solution was stirred for 4 hours and washed 3 times, followed by the addition of DI and sonication for 1 hour. The mixing was separated through centrifugation (3500 rpm, 10 min) and the precipitate was collected as h-$Ti_3C_2T_x$ slurry.

Synthesis of TiO_2 thin film

A PVP solution with a concentration of 7 wt% was prepared from PVP powders and alcohol with stirring. Another solution well mixed 2.95 mL titanium (IV) isopropoxide, 1.7 mL acetate and 1.75 mL anhydrous ethanol. The two solutions were mixed and stirred for several minutes. Then the precursor solution was transferred into a syringe and pushed at a flow rate of 6 mL h^{-1}. The positive voltage applied to the needle of the syringe was 10 kV and the distance between the needle tip and the collector was 15 cm. The resulting free-standing white thin film on the Al foil was then calcinated at 600℃ for 2 hours and peeled off from the Al foil.

Photodetector integration

A slit was made in the processed leaf and slurry of m-$Ti_3C_2T_x$ and h-$Ti_3C_2T_x$ were coated on both sides of the leaf. When the MXenes were still wet, TiO_2 thin film was placed onto it and given a press to hold the leaf and TiO_2 film together. Then the photodetector was dried in a hot plate. To ensure its strength during bending tests, a tiny amount of PDMS was coating on its surface and cured at 60℃.

Characterization and measurements

The sample morphologies were characterized by field-emitting scanning electron microscope (Zeiss Sigma). Transmission electron microscopy analyses were conducted by a JEM-2010 electron microscope (JEOL, Japan). X-ray photoelectron spectroscopy tests were carried out on an electron spectrometer (Thermo Scientific K-Alpha$^+$). X-ray diffraction patterns were recorded on a Bruker D8-A25 diffractometer using Cu Kα radiation (λ = 1.5405 Å). UV-vis transmittance spectra were obtained using a UV-vis spectrometer (Hitachi U-3900H). Raman spectroscopy was conducted by Dilor LabRam-1B via He-Ne laser of 4 mW with excitation wavelength of 532 nm. Ultraviolet photoelectron spectroscopy measurement was done via a Specs UVLS using He I excitation (21.22 eV). The sheet resistance was measured according to the methods in literature.[2] The leaf electrodes were cut into 1.5 cm×1 cm pieces and silver paste were coated on the edges. The sheet resistance was measured by Fluke 87V multimeter and calculated as:

$$R_s = R\frac{W}{L}$$

where R was measured resistance, W and L referred to the width and length of samples. The optoelectronic properties were collected with the semiconductor characterization system (Keithley 4200-SCS) and a 70 W xenon arc lamp with a monochromator was used as light source. The light intensity was measured with a NOVA II power meter (OPHIR photonics). All the measurements were performed at room temperature.

S2. Morphology and electrical resistance of bio-inspired electrodes

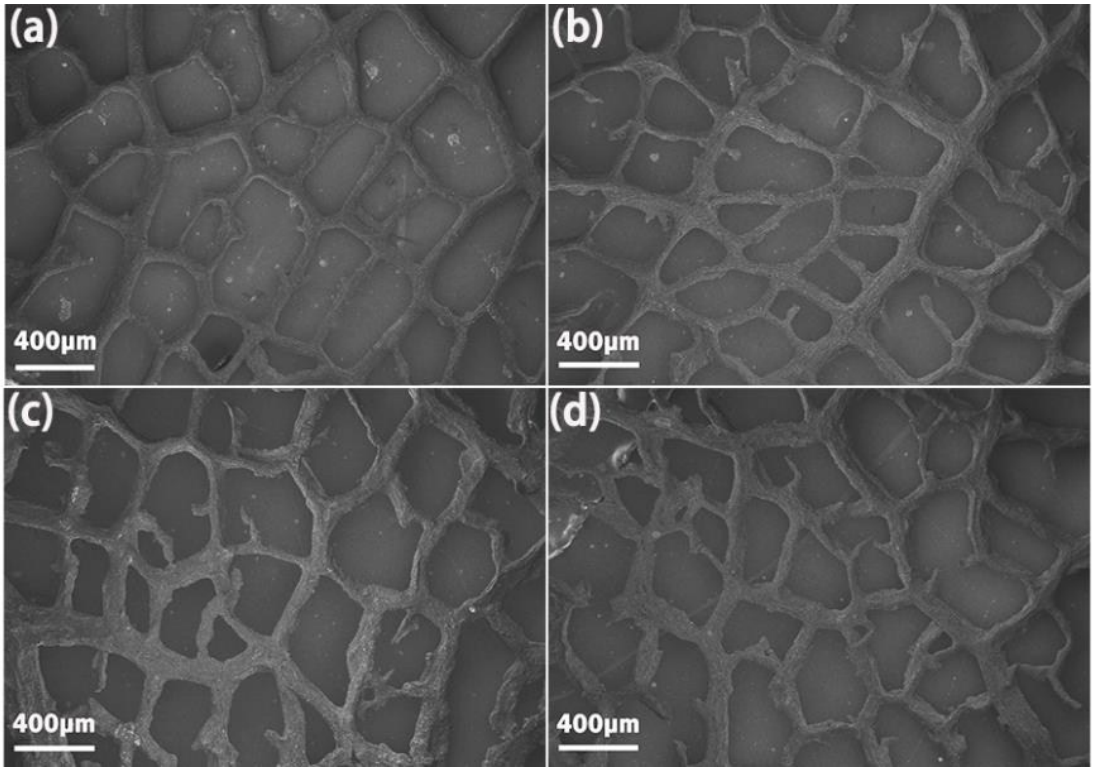

Fig. S1. The SEM images of the leaf electrode after coating m-$Ti_3C_2T_x$ for a) 2, b) 4, c) 6, d) 8 times.

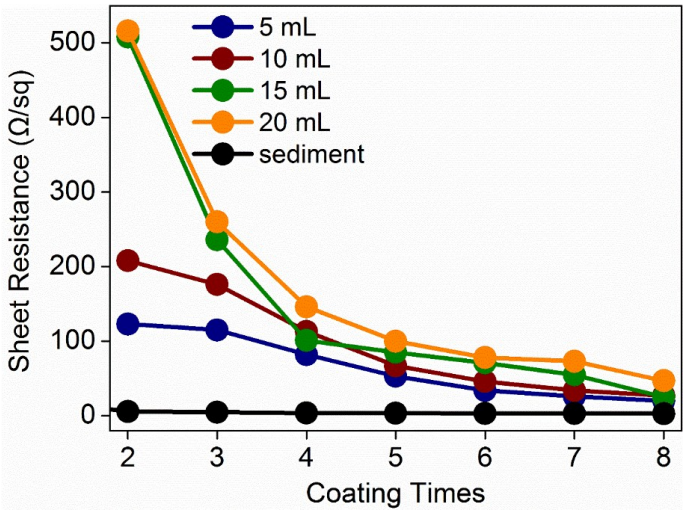

Fig. S2. The sheet resistance values of leaf electrodes coated with m-$Ti_3C_2T_x$ slurry (sediment) or solutions for different coating times.

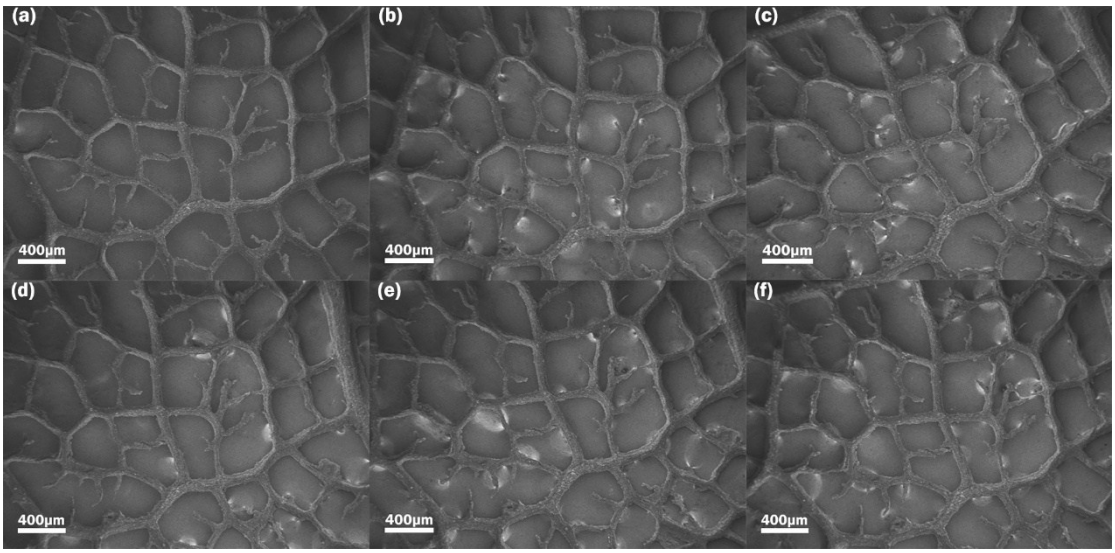

Fig. S3. The SEM images of the leaf electrode after being bent for a) 0, b) 200, c) 400, d) 600, e) 800, f) 1000 times.

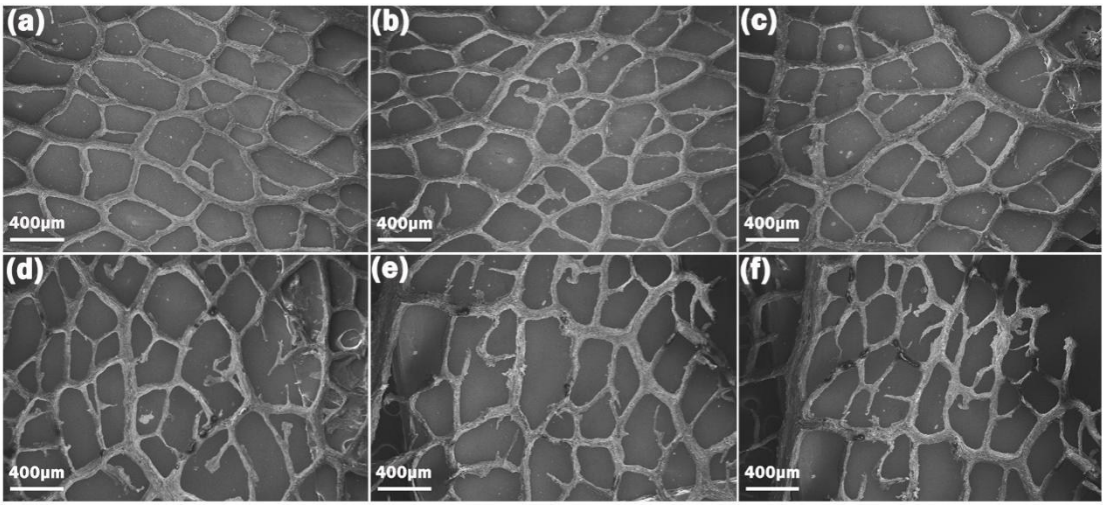

Fig. S4. The SEM images of Scotch-tape tests for a) 0, b) 10, c) 20, d) 30, e) 40, f) 50 times.

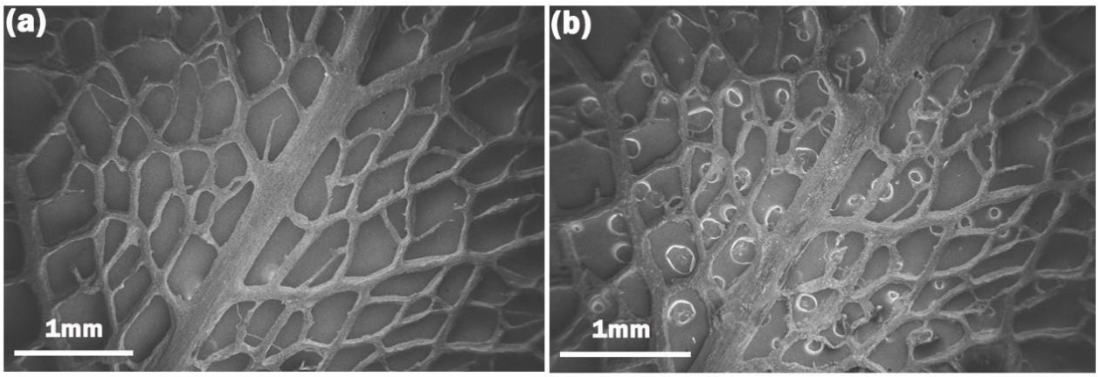

Fig. S5. The SEM images of the leaf electrode at the same position a) before crumpling and b) after unfolding. The circles on b) were the trails of crumpling.

S3. Characterization of electrospun TiO_2

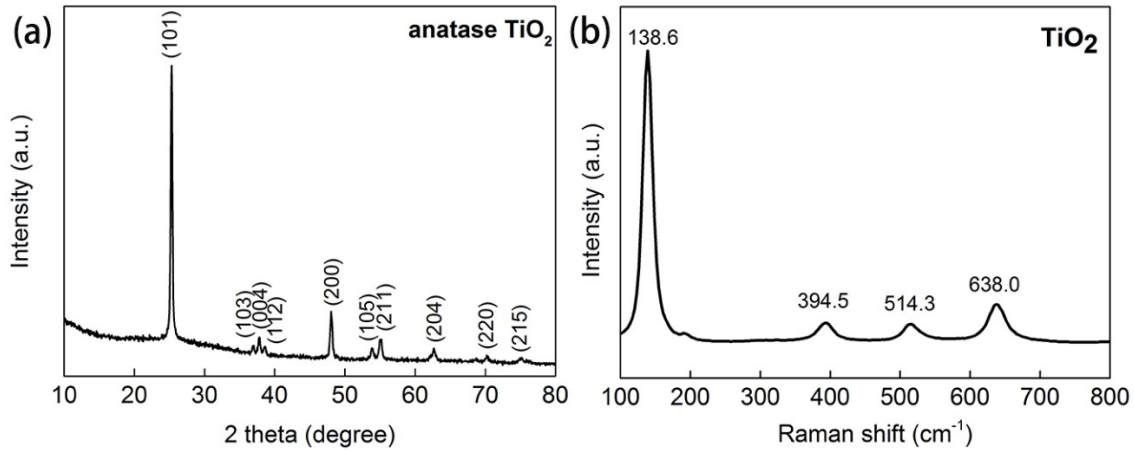

Fig. S6. The XRD results and Raman spectra of TiO_2.

S4. Morphology and transmittance of h-$Ti_3C_2T_x$ electrodes

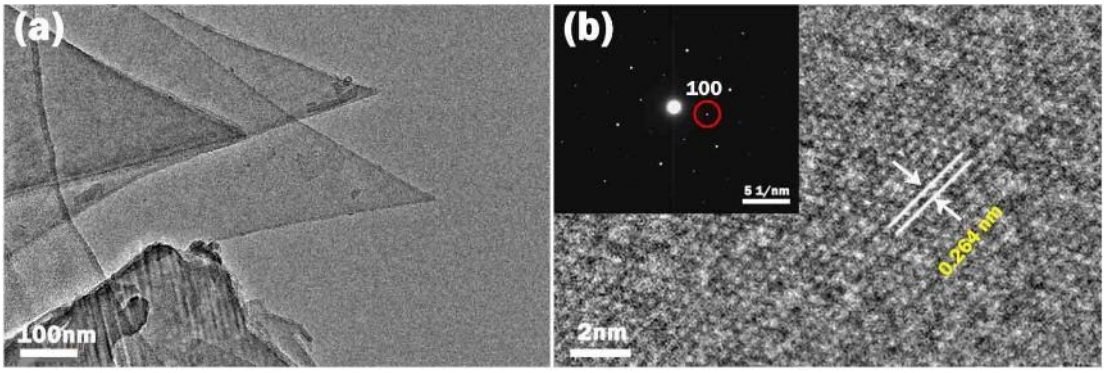

Fig. S7. The TEM, HRTEM and SAED results of few-layer h-$Ti_3C_2T_x$.

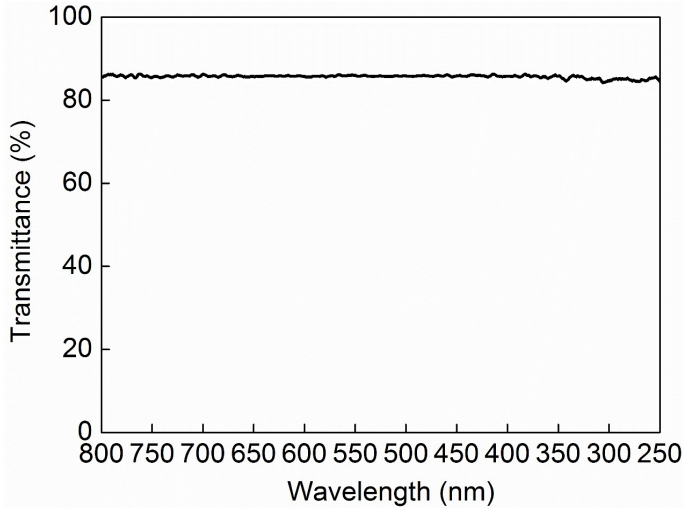

Fig. S8. The transmittance of the leaf electrode coated with h-$Ti_3C_2T_x$ for one time.

S5. Characterization of m-$Ti_3C_2T_x$ and h-$Ti_3C_2T_x$

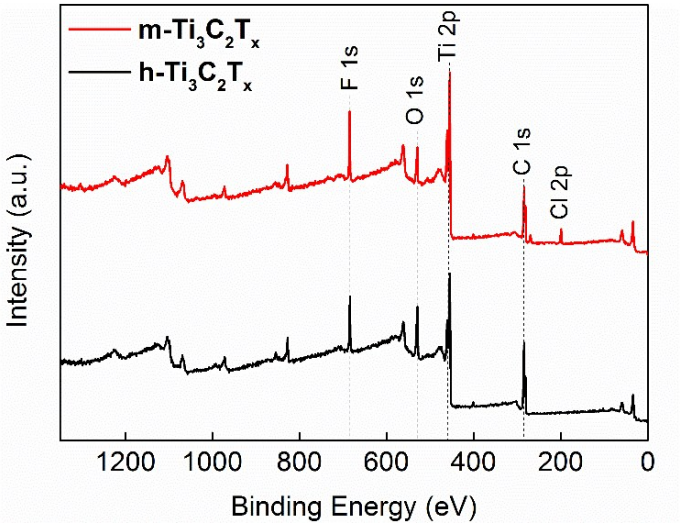

Fig. S9. XPS spectra of m-$Ti_3C_2T_x$ and h-$Ti_3C_2T_x$ in the all elements regions.

The Cl 2p peak in m-$Ti_3C_2T_x$ curve results from the small amount of -Cl on the MXene surface.

Table S1. Atomic percent in m-$Ti_3C_2T_x$ and h-$Ti_3C_2T_x$ obtained by XPS analysis.

Atomic Percent (%)	**Ti 2p**	**C 1s**	**O 1s**	**F 1s**	**Cl 2p**
m-$Ti_3C_2T_x$	25.11	45.17	11.96	13.72	4.05
h-$Ti_3C_2T_x$	20.45	52.01	16.08	11.46	-

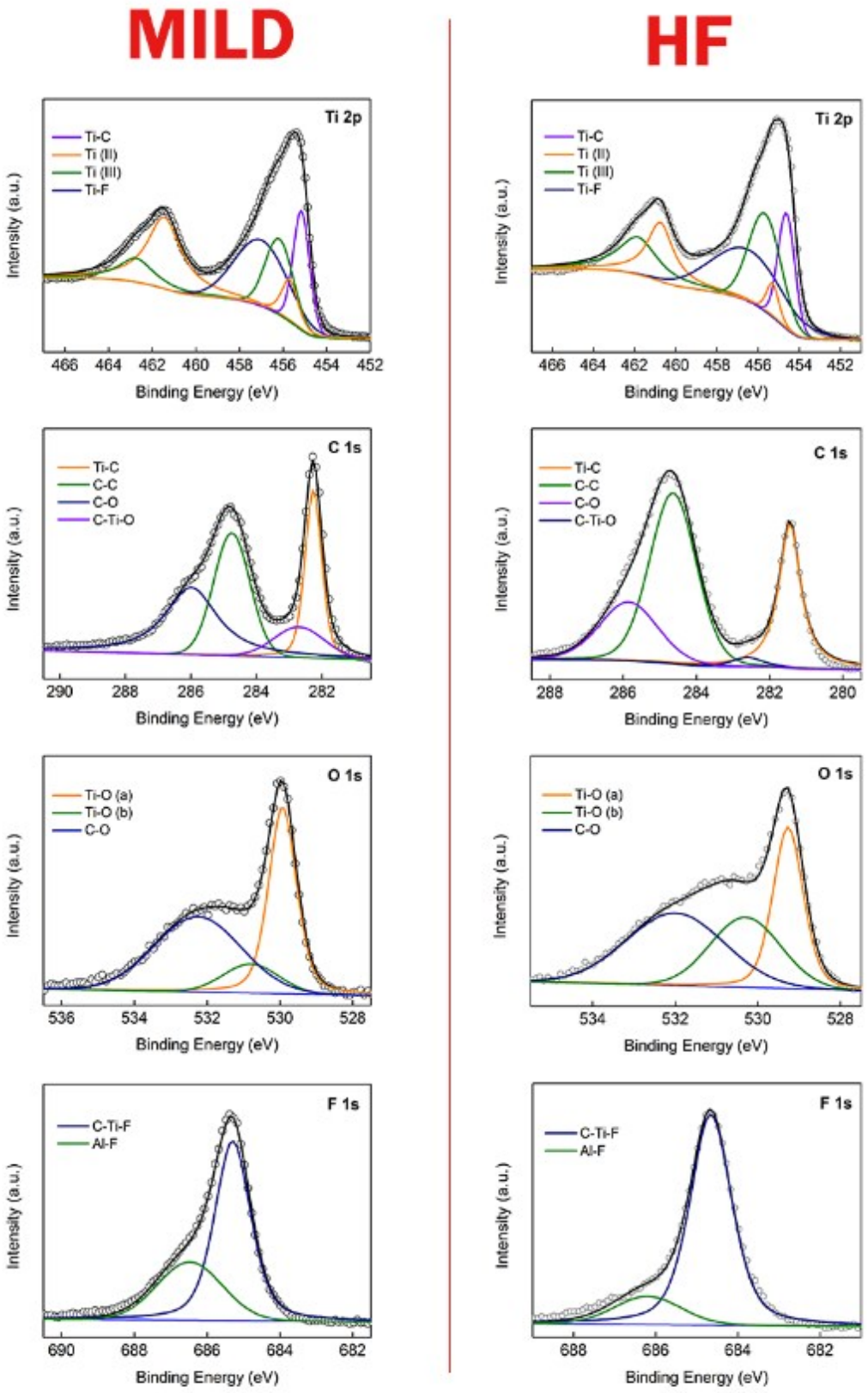

Fig. S10. The high resolution XPS results of m-$Ti_3C_2T_x$ (MILD in the figure) and h-$Ti_3C_2T_x$ (HF in the figure).

High resolution XPS spectrum in Figure S10 of Ti 2p confirms the presence of Ti atoms bonded to C at about 455.0 eV, whereas Ti(II) and Ti(III) atoms bonded with -O or -OH at 455.6 eV (461.2 eV) and 456.1 eV (462.4 eV).[3] The Ti-O bonding is also confirmed by O 1s peaks at around 529.7 and 530.6 eV, where the two demonstrate oxygen at different sites.[4] The Ti 2p peak at about 457.0 eV stems from Ti-F, which is also evidenced by the F 1s peak at 685.1 eV. The peak at 686.5 eV of Al-F bonding originates from etching of MAX phase. [5] The C 1s peak at 282.0 eV indicates Ti-C bonding, one from 284.8 eV is from C-C contaminations and one from 285.8 eV indicates C-O bonding while 282.7 eV C-Ti-O bonding.[5] C-O bonding is also confirmed by O 1s peak at 532.2 eV. Particularly, there is a slight 0.7 eV shift of h-$Ti_3C_2T_x$ Ti 2p peaks to higher energy compared with m-$Ti_3C_2T_x$ Ti 2p peaks. This may result from the slight difference between the surface terminal groups of two kinds of $Ti_3C_2T_x$, which needs detailed characterization in the future.

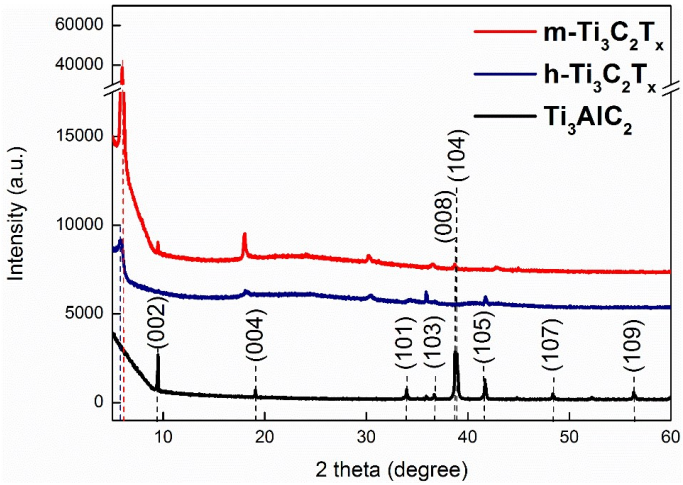

Fig. S11. The XRD data of m-$Ti_3C_2T_x$ and h-$Ti_3C_2T_x$.

XRD pattern of Ti_3AlC_2 powder shows characteristic (00*l*) peaks with (002) peak at 9.5° corresponding to a *c*-lattice parameter of 20.8 Å.[6] After etching and dried in vacuum, the obtained $Ti_3C_2T_x$ film shows almost only one intensive (002) peak with an increased intensity at 6.0° (m-$Ti_3C_2T_x$) and 5.7° (h-$Ti_3C_2T_x$), indicating a *d*-spacing of 14.7 Å (m-$Ti_3C_2T_x$) and 15.8 Å (h-$Ti_3C_2T_x$) as well as highly c-oriented restacking nature of $Ti_3C_2T_x$ films.[7] The peak shift confirms the increased d-spacing during Li^+ or TBAOH intercalation between $Ti_3C_2T_x$ layers. The disappeared main diffractions of (008) and (104) (2θ of 38.7°and 39.0°, respectively) in $Ti_3C_2T_x$ compared with MAX phase, demonstrate the successful removal of Al elements during two kinds of etching processes.

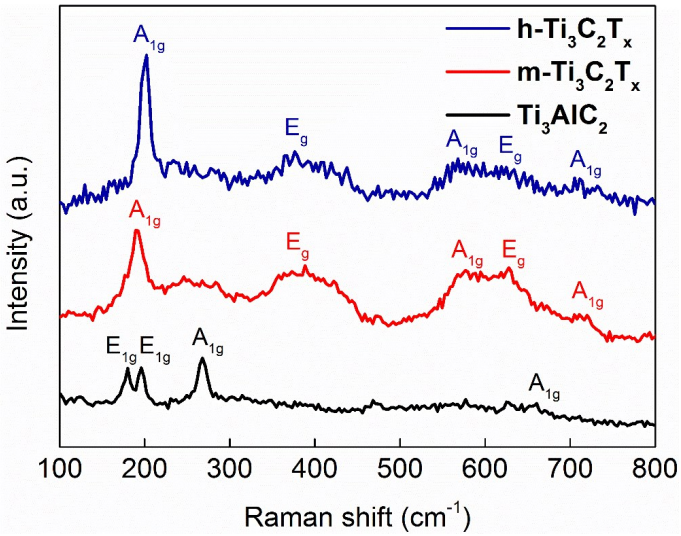

Fig. S12. The Raman spectra of m-$Ti_3C_2T_x$ and h-$Ti_3C_2T_x$.

For $Ti_3C_2T_x$ spectra, the peaks at about 191 and 473 cm^{-1}can be assigned to A_{1g} modes of $Ti_3C_2F_2$. Other peaks can be considered as A_{1g} of $Ti_3C_2O_2$ (719 and 577 cm^{-1}), E_g of $Ti_3C_2O_2$ (372 cm^{-1}), E_g of $Ti_3C_2(OH)_2$ (282 and 628 cm^{-1}), A_{1g} of $Ti_3C_2(OH)_2$ (247 cm^{-1}).[8] The broader spectrum compared with Ti_3AlC_2 and these peaks indicate the success synthesis of $Ti_3C_2T_x$ and the presence of surface functional group atoms.[7, 9] There is no titanium oxide peak around 144 cm^{-1}, showing no sense of oxidation.[10]

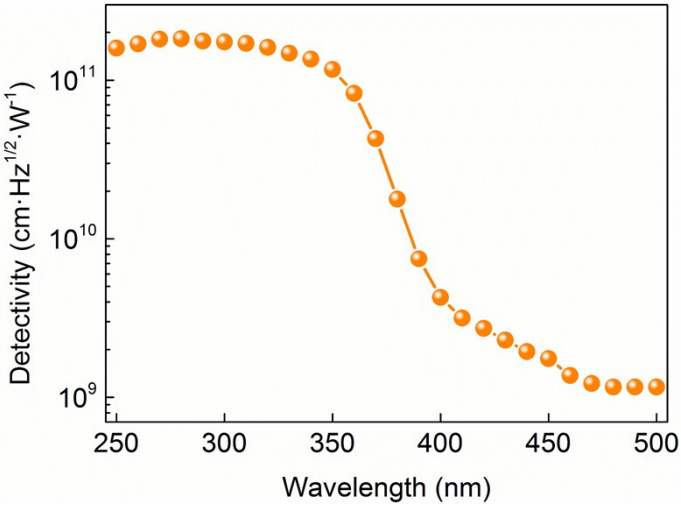

Fig. S13. The detectivity (D^*) of the bio-inspired photodetector.

The detectivity was calculated as $D^* = R_\lambda/(2qJ_d)^{1/2}$, where R_λ refers to responsivity of the photodetector, q is the element charge and J_d is dark current density.[11]

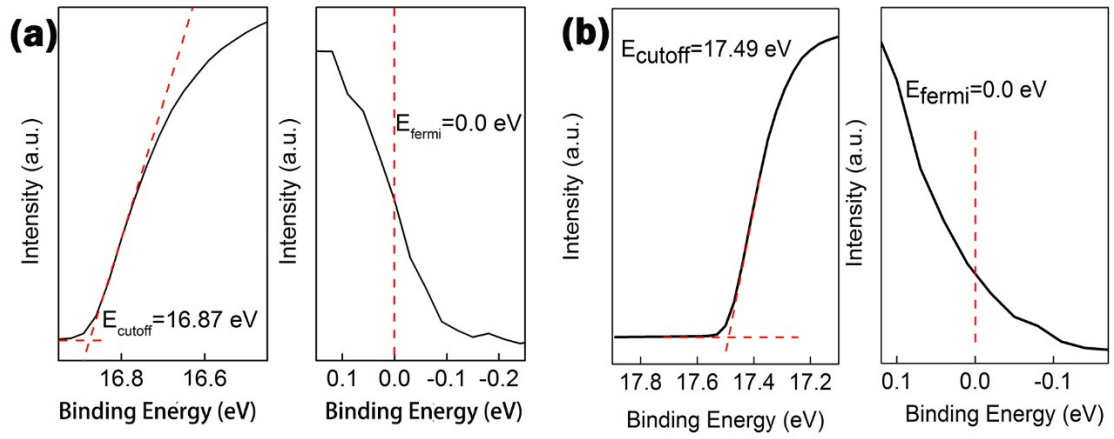

Fig. S14. The UPS results of a) m-$Ti_3C_2T_x$ and b) h-$Ti_3C_2T_x$.

S6. Electrical measurements of m-$Ti_3C_2T_x$ and h-$Ti_3C_2T_x$

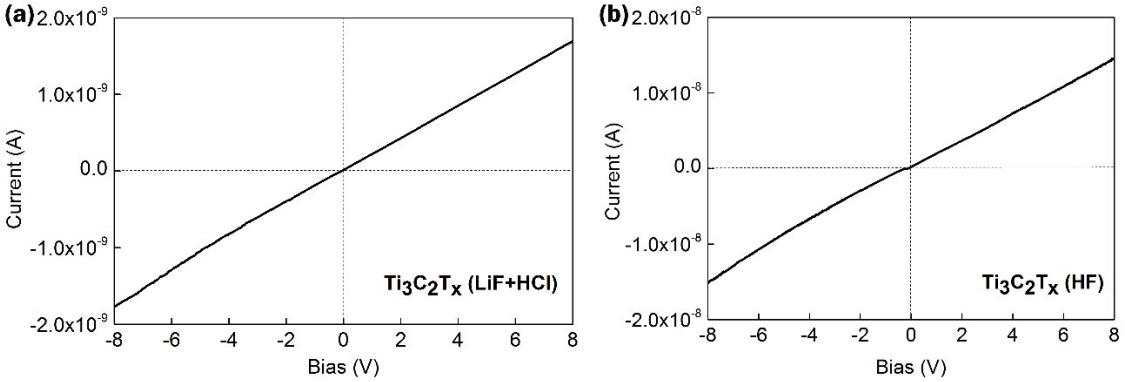

Fig. S15. The *I-V* curves of TiO_2 with a) m-$Ti_3C_2T_x$ and b) h-$Ti_3C_2T_x$ as symmetric electrodes, respectively.

References:

(1) Alhabeb, M.; Maleski, K.; Anasori, B.; Lelyukh, P.; Clark, L.; Sin, S.; Gogotsi, Y. Guidelines for Synthesis and Processing of Two-Dimensional Titanium Carbide ($Ti_3C_2T_x$ MXene). *Chem. Mater.* **2017,** *29*, 7633-7644.

(2) Tian, W.; VahidMohammadi, A.; Wang, Z.; Ouyang, L.; Beidaghi, M.; Hamedi, M. M. Layer-by-layer self-assembly of pillared two-dimensional multilayers. *Nat. Commun.* **2019,** *10*, 2558.

(3) Agresti, A.; Pazniak, A.; Pescetelli, S.; Di Vito, A.; Rossi, D.; Pecchia, A.; Auf der Maur, M.; Liedl, A.; Larciprete, R.; Kuznetsov, D. V.; Saranin, D.; Di Carlo, A. Titanium-carbide MXenes for work function and interface engineering in perovskite solar cells. *Nat. Mater.* **2019,** *18*, 1228-1234.

(4) Persson, I.; Näslund, L.-Å.; Halim, J.; Barsoum, M. W.; Palisaitis, J.; Rosen, J.; Persson, P. O. Å. On the organization and thermal behavior of functional groups on Ti_3C_2 MXene surfaces in vacuum. *2D Mater.* **2018,** *5*, 015002.

(5) Physical Chemistry Chemical PhysicsSchultz, T.; Frey, N. C.; Hantanasirisakul, K.; Park, S.; May, S. J.; Shenoy, V. B.; Gogotsi, Y.; Koch, N. Surface Termination Dependent Work Function and Electronic Properties of $Ti_3C_2T_x$ MXene. *Chem. Mater.* **2019,** *31*, 6590-6597.

(6) Yasaei, P.; Hemmat, Z.; Foss, C. J.; Li, S. J.; Hong, L.; Behranginia, A.; Majidi, L.; Klie, R. F.; Barsoum, M. W.; Aksamija, Z.; Salehi-Khojin, A. Enhanced Thermal Boundary Conductance in Few-Layer Ti_3C_2 MXene with Encapsulation. *Adv. Mater.* **2018,** *30*, 1801629.

(7) Wang, Z.; Kim, H.; Alshareef, H. N. Oxide Thin-Film Electronics using All-MXene Electrical Contacts. *Adv. Mater.* **2018,** *30*, 1706656.

(8) Hu, T.; Wang, J.; Zhang, H.; Li, Z.; Hu, M.; Wang, X. Vibrational properties of Ti_3C_2 and $Ti_3C_2T_x$ (T=O, F, OH) monosheets by first-principles calculations: a comparative study. *Phys. Chem. Chem. Phys.* **2015,** *17*, 9997-10003.

(9) Tu, S.; Jiang, Q.; Zhang, X.; Alshareef, H. N. Large Dielectric Constant Enhancement in MXene Percolative Polymer Composites. *ACS Nano* **2018,** *12*, 3369-3377.

(10) Fu, H. C.; Ramalingam, V.; Kim, H.; Lin, C. H.; Fang, X.; Alshareef, H. N.; He, J. H. MXene-Contacted Silicon Solar Cells with 11.5% Efficiency. *Adv. Energy Mater.* **2019,** *9*, 1900180.

(11) Zhao, B.; Wang, F.; Chen, H.; Wang, Y.; Jiang, M.; Fang, X.; Zhao, D. Solar-Blind Avalanche Photodetector Based On Single ZnO-Ga_2O_3 Core-Shell Microwire. *Nano Lett.* **2015**, *15*, 3988-3993.